



Kent Academic Repository

Tröster, Tobias, Endres, Franziska, Arrowsmith, Merle, Endres, Lukas, Fantuzzi, Felipe and Braunschweig, Holger (2023) *Dibenzoberylloles: antiaromatic s-block fluorene analogues*. *Chemical Communications*, 59 (60). pp. 9199-9202. ISSN 1359-7345.

Downloaded from

<https://kar.kent.ac.uk/102067/> The University of Kent's Academic Repository KAR

The version of record is available from

<https://doi.org/10.1039/D3CC02736H>

This document version

Author's Accepted Manuscript

DOI for this version

Licence for this version

UNSPECIFIED

Additional information

Versions of research works

Versions of Record

If this version is the version of record, it is the same as the published version available on the publisher's web site. Cite as the published version.

Author Accepted Manuscripts

If this document is identified as the Author Accepted Manuscript it is the version after peer review but before type setting, copy editing or publisher branding. Cite as Surname, Initial. (Year) 'Title of article'. To be published in **Title of Journal**, Volume and issue numbers [peer-reviewed accepted version]. Available at: DOI or URL (Accessed: date).

Enquiries

If you have questions about this document contact ResearchSupport@kent.ac.uk. Please include the URL of the record in KAR. If you believe that your, or a third party's rights have been compromised through this document please see our [Take Down policy](https://www.kent.ac.uk/guides/kar-the-kent-academic-repository#policies) (available from <https://www.kent.ac.uk/guides/kar-the-kent-academic-repository#policies>).

COMMUNICATION

Dibenzoberylloles: antiaromatic s-block fluorene analogues

Tobias Tröster,^{a,b} Franziska Endres,^{a,b} Merle Arrowsmith,^{a,b} Lukas Endres,^{a,b} Felipe Fantuzzi,^c and Holger Braunschweig^{*,a,b}Received 00th January 20xx,
Accepted 00th January 20xx

DOI: 10.1039/x0xx00000x

Among a series of Lewis base-stabilised antiaromatic dibenzoberylloles (DBBs) the cyclic alkyl(amino)carbene (CAAC) analogue undergoes a complex but highly selective thermal decomposition, involving the breaking and making of four bonds each, which yields a rare beryllium η^2 -alkene complex. Two-electron reduction of the CAAC-stabilised DBBe analogue yields an aromatic dianion.

Dibenzoboroles (I, Fig.), also known as 9-borafluorenes, have been receiving increased attention over the last two decades.¹ Comprised of a central five-membered BC₄ borole ring (II) featuring four π electrons,² they are benzo-fused on both sides, providing them with additional electronic stabilisation through π delocalisation. Dibenzoboroles may also be viewed as boron analogues of the fluorenyl cation, in which the C9 carbon atom has been replaced by an isolobal trigonal-planar boron centre with a vacant p orbital. Both the antiaromatic character of the central BC₄ ring and the extended conjugation give rise to unusual optical properties and varied reactivity.³ These characteristics, combined with a small HOMO-LUMO gap, have found applications in optoelectronic materials such as organic light-emitting diodes (OLEDs)⁴ and organic solar cells (OSCs).⁵

While a handful of alkaline earth analogues of boroles, in which a group 2 element takes the place of the boron atom, have been reported, their annelated counterparts remain unknown. The first examples of magnesacyclopentadienes (or magnesoles) were synthesised *in situ* by the group of D'yakonov in 2007, but their structure was not confirmed by X-ray crystallographic analysis.⁶ In 2014 Xi obtained the first stable magnesole, complex III.⁷ More recently, we reported the synthesis of the lighter, cyclic alkyl(amino)carbene (CAAC)-stabilised, beryllole homologue IV,⁸ the first beryllium

heterocycle to exhibit significant antiaromaticity, albeit to a lesser degree than the isoelectronic borole II.

Given the interesting optoelectronic properties and reactivity of benzannulated boroles, we aimed to synthesise a range of dibenzoberylloles (DBBs) to study their electronic structure and reactivity.

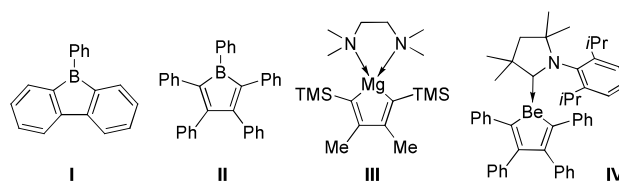
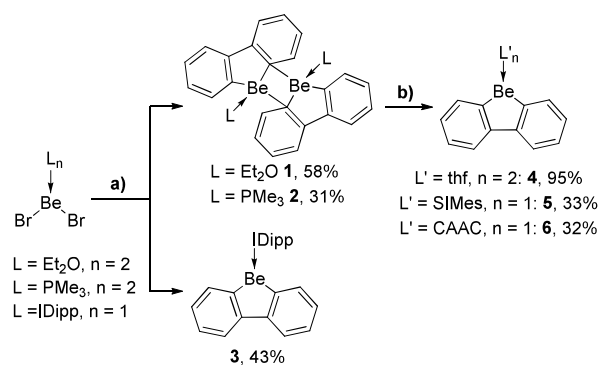


Figure 1. Selected examples of a 9-borafluorene (I), a borole (II), a magnesole (III), and a beryllole (IV). TMS = trimethylsilyl.



Scheme 1. Syntheses of DBBs 1-6; a) 1 equiv. 2,2'-dilithiobiphenyl, toluene, rt, 16 h; b) for L = Et₂O: L' = thf, solvent = THF, 80 °C 16 h; L' = SIMes, CAAC, solvent = C₆H₆, rt, 16 h. IDipp = 1,3-bis(2,6-diisopropylphenyl)imidazol-2-ylidene; SIMes = 1,3-bis(2,4,6-trimethylphenyl)-4,5-dihydroimidazol-2-ylidene; CAAC = 1-(2,6-diisopropylphenyl)-3,3,5,5-tetramethylpyrrolidin-2-ylidene.

^a Institute for Inorganic Chemistry, Julius-Maximilians-Universität Würzburg, Am Hubland, 97074 Würzburg (Germany)

^b Institute for Sustainable Chemistry & Catalysis with Boron, Julius-Maximilians-Universität Würzburg, Am Hubland, 97074 Würzburg (Germany)

^c School of Chemistry and Forensic Science, University of Kent, Park Wood Rd, Canterbury, CT2 7NH (United Kingdom)

Electronic Supplementary Information (ESI) available: Synthetic procedures, NMR and IR spectra, X-ray crystallographic and computational details. CCDC 2253157-2253164. For ESI and crystallographic data in CIF or other electronic format see DOI: 10.1039/x0xx00000x

Lewis-base-stabilised DBBs were obtained by salt metathesis of 2,2'-dilithium-biphenyl with Lewis-base-stabilised beryllium dibromides (L_nBeBr₂; L = Et₂O, PMe₃, n = 2; L = IDipp 1,3-bis(2,6-diisopropylphenyl)imidazol-2-ylidene, n = 1, Scheme 1a).[†] The ⁹Be NMR resonances of 1 and 2 are very similar in chemical shift and broadness (1: 10.8 ppm, full width at mid-

height (fwmh) \approx 120 Hz; **2**: 8.2 ppm, fwmh \approx 100 Hz), while that of **3** is somewhat downfield-shifted and significantly broader (14.5 ppm, fwmh \approx 380 Hz), reflecting the tetracoordinate nature of **1** and **2** and tricoordinate nature of **3** in solution.⁹

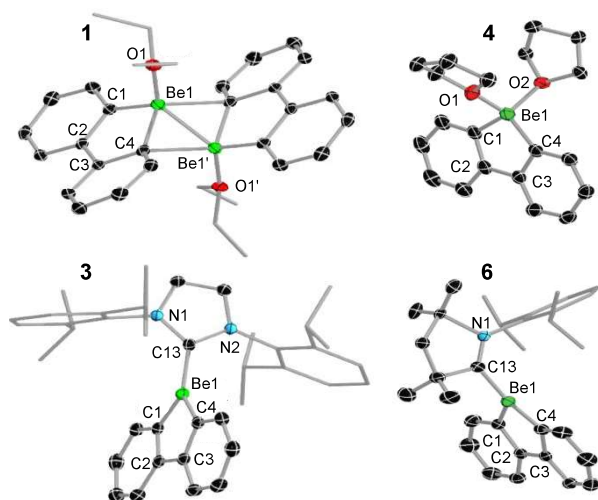
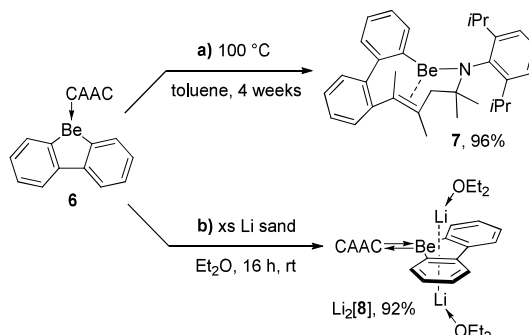


Figure 2. Solid-state structures of **1**, **3**, **4** and **6** with atomic displacement ellipsoids shown at the 50% probability level. All H atoms and ellipsoids of ligand periphery are omitted for clarity.

X-ray structural analyses (Fig. 2 and Fig. S26 in the ESI) show that **1** and **2** are dimeric in the solid state, whereas **3** is monomeric. The dimers feature tetrahedral beryllium atoms, with endocyclic Be–C bond lengths (**1** 1.760(3) Å; **2** 1.758(3) Å) comparable to that of the non-annulated beryllole **IV** (1.763(2) Å).⁸ The Be...Be distances (**1** 2.106(3) Å; **2** 2.044(4) Å) are within the typical range of electron-deficient organyl-bridged beryllium oligomers (2.03–2.33 Å).¹⁰ The C–C bond length alternation in the central BeC₄ ring (avg. C1–C2/C3–C4 1.42 Å; avg. C2–C3 1.49 Å) is less marked than in borfluorene **I** (avg. C1–C2/C3–C4 1.43 Å; C2–C3 1.512(11) Å) or beryllole **IV** (C1–C2/C3–C4 (avg.) 1.36 Å, C2–C3 1.512(2) Å),⁸ suggesting a higher degree of π delocalisation in complexes **1–3**.¹¹ The purely σ -donating Be–C_{IDipp} bond in **3** (1.788(2) Å) is longer than the covalent Be1–C1/4 bonds (avg. 1.75 Å) and significantly longer than the Be–C_{NHC} bonds (NHC = N-heterocyclic carbene) reported in other (NHC)BeR₂ adducts (1.79–1.82 Å).¹²

Taking advantage of the lability of the Et₂O ligand in **1** three more DBBes were obtained by exchange with stronger Lewis bases: THF, SIMes (1,3-bis(2,4,6-trimethylphenyl)-4,5-dihydroimidazol-2-ylidene) and CAAC (1-(2,6-diisopropylphenyl)-3,3,5,5-tetramethylpyrrolidin-2-ylidene, Scheme 1b).[†] The ⁹Be NMR spectrum of **4** exhibits a sharp singlet at 13.2 ppm (fwmh \approx 80 Hz), indicative of a four-coordinate beryllium centre, in this case bearing two THF ligands (Fig. 2). Relative to that of **4**, the ⁹Be NMR resonances of compounds **5** and **6** are significantly downfield-shifted to 24.3 (**5**) and 23.6 (**6**) ppm and exhibit strong broadening (fwmh \approx 320–380 Hz), typical of tricoordinate beryllium compounds. The lower electron density at beryllium compared to **3** may be owed to the substantial π -accepting nature of SIMes and CAAC. X-ray diffraction analyses confirmed the nuclearity and geometry of **4–6** (Fig. 2 and Fig. S27 in the ESI). While the steric demands of the individual coordinated Lewis bases in complexes **1–6** impact the nuclearity and coordination

number at beryllium, the bonding parameters within the DBBe framework remain virtually identical, except for those of **4**, in which the endocyclic Be–C bonds are elongated to 1.784(3) Å due to the higher coordination number, comparable to that in [(thf)₂Be(Ter^{Mes})(OCMnCp(CO)₂)] (1.782(5) Å; Cp = C₅H₅, Ter^{Mes} = 2,6-dimesitylphenyl).¹³



Scheme 2. Thermal decomposition and twofold reduction of **6**.

Heating a toluene solution of **6** to 100 °C for four weeks led to its selective decomposition to complex **7**, isolated as a colourless solid in 96% yield (Scheme 2a), with a ⁹Be NMR shift of 14.3 ppm (fwmh \approx 360 Hz). The ¹H NMR spectrum shows a highly unsymmetrical CAAC backbone with four distinct methyl singlets at 2.06, 1.78, 1.37 and 1.14 ppm. X-ray crystallographic analysis revealed that a double ring expansion, of both the CAAC and the beryllole rings, had occurred (Fig. 3a). The central ten-membered C₈BeN heterocycle results from a complex, multi-step rearrangement including shifting of the beryllium atom from C_{carbene} to the adjacent nitrogen atom, cleavage of the N–C_{carbene} bond and one endocyclic beryllole Be–C bond, formation of a new C–C bond between the former C_{carbene} atom and the C2 position of the pendant biphenyl moiety, and lastly a methyl group shift to the adjacent former C_{carbene} atom. To our knowledge there are only a few known examples of CAAC ring-opening reactions, none of which include methyl group shifts.^{14–16} This reaction is all the more remarkable in that it involves breaking two Be–C bonds as well as strong N–C and C–C single bonds, whilst forming two new C–C single bonds and a covalent Be–N bond, i.e. a total of eight bonds broken or formed, in a completely selective fashion and near-quantitative yield.

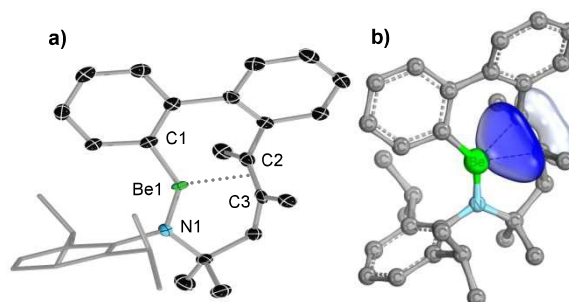


Figure 3. a) Solid-state structure of **7** with atomic displacement ellipsoids shown at the 50% probability level (left). All H atoms are omitted for clarity. Selected distances [Å] and angles [°]: Be1–N1 1.548(4), Be1–C1 1.716(4), C2–C3 1.354(4), Be1... (mid-point C2=C3) 1.999(4), Be1–C2 2.111(4), Be1–C3 2.126(4), C1–Be1–N1 139.1(3); b) IBO featuring the interaction between the alkene moiety and the beryllium atom (isosurface encloses 80% of the orbital electron density).

The newly formed Be–N (1.548(4) Å) and Be–C (1.716(4) Å) bonds of **7** are within the typical range for single bonds in dicoordinate beryllium complexes (Be–N 1.52–1.54 Å; Be–C 1.70 Å).^{13,17} The methyl group shift results in an alkene moiety, which engages in a side-on π interaction with the beryllium centre, leading to significant bending of the C1–Be1–N1 motif (139.1(3)°) and an elongation of the C=C double bond (1.354(4) Å), relative to conventional olefins (e.g. 2,3-dimethylbutadiene: 1.23 Å).¹⁸ The Be \cdots (alkene) distance of ca. 2.00 Å is much longer than in the only other known beryllium π complex, a beryllium-bridged naphthalene-1,4-diyl π complex (ca. 1.73 Å).¹⁹ Compound **7** contains a far more loosely-tethered Be \cdots olefin interaction, suggesting a more "natural" (i.e. less geometry-enforced) Be \cdots alkene π interaction.

This unique structure prompted us to quantify the Be \cdots C₂ interaction computationally. The intrinsic bond orbital (IBO)²⁰ analysis supports the existence of a Be \cdots alkene orbital interaction (Fig. 3b), which is, however, primarily centred at the alkene moiety (97%), leaving a mere 3.0% on the beryllium atom itself. The Mayer bond orders (Be1–C2: 0.20, Be1–C3: 0.17), fuzzy bond orders (Be1–C2: 0.26, Be1–C3: 0.23), Wiberg bond indices (Be1–C2: 0.26, Be1–C3: 0.24) and natural binding indices (Be1–C2: 0.22, Be1–C3: 0.18) were calculated to evaluate the magnitude of this interaction, further endorsing the presence of a weak beryllium π complex. In summary, the structural parameters, together with quantum-chemical methods, show that compound **7** indeed exhibits a non-negligible, albeit modest, beryllium \cdots alkene π interaction.

Twofold reduction of **6** with lithium sand in diethyl ether provided complex Li₂[**8**] as a highly air- and temperature-sensitive dark purple crystalline solid (Scheme 2b). The ⁹Be NMR resonance of Li₂[**8**] (7.6 ppm, fwhm \approx 155 Hz) is significantly upfield-shifted from and sharper than that of **6** (23.6 ppm, fwhm \approx 320 Hz), indicating a higher electron density at the tricoordinate beryllium atom, as expected upon reduction. X-ray diffraction analysis confirmed the η^4 coordination of two lithium etherate moieties on each side of the central BeC₄ ring (Fig. 4a). This structural motif resembles that of the dianion of **IV**, which displays some aromaticity,⁸ and that of the 9H-9-borafluorene dianion reported by Wagner.²¹

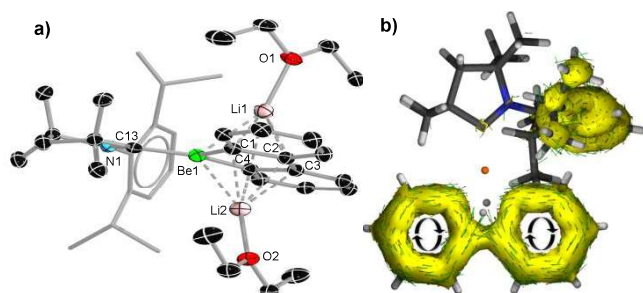


Figure 4. a) Molecular structure of Li₂[**8**] with atomic displacement ellipsoids shown at 50% probability level. All H atoms are omitted for clarity; b) Acid plot of Li₂[**8**].

The Be–C_{CAAC} bond of Li₂[**8**] (1.709(2) Å), shorter than that of **6** by ca. 0.08 Å, is now shorter than the endocyclic Be–C bonds (avg. 1.77 Å). This may be explained by π backdonation from the electron-rich beryllium centre to the π -acidic CAAC ligand, which is further supported by the nearly coplanar arrangement of the carbene π framework and the reduced DBBe ligand (torsion angle C1–Be1–C13–N1 167.4(1)°) and an elongation of

the C_{CAAC}–N bond by 0.067 Å. Both endocyclic Be–C bonds show a slight elongation compared to those of **6** (ca. 0.01 Å) and thus indicate Be–C single bonds. The C–C bonds in the BeC₄ ring exhibit bond length equalisation to ca. 1.46 Å, in line with the formal aromatisation of the ring system. In contrast, the analogous dianion of **IV** shows a shortening of the endocyclic Be–C bonds (ca. 0.03 Å). Moreover, the higher C–Be–C–N torsion angle (94.2(3)°) in **IV** prevents π backdonation to the CAAC moiety in this species, as seen in the longer Be–C_{CAAC} bond (1.817(2) Å) and the increased C–C bond length alternation in the BeC₄ ring (C1–C2/C3–C4 (avg.) 1.47 Å, C2–C3 1.4482(18) Å).⁸ To further investigate the electronic structure of Li₂[**8**], restricted and broken-symmetry DFT calculations were performed at the (U)wB97X-D/6-311++G(d,p) level and the complete active space self-consistent field (CASSCF) method (see ESI for details). Li₂[**8**] exhibits a closed-shell singlet (CSS) ground state, with large vertical/adiabatic singlet-triplet (S–T) gaps of 17.8/12.8 kcal mol^{–1} according to DFT calculations. Inspection of the CASSCF orbitals and occupancies also supports a CSS ground state. In contrast, the bare dianion [**8**]^{2–} is an open-shell species with a triplet (OST) ground state and a low-lying open-shell singlet (OSS) state ($\Delta E(\text{OS–T}) = 0.04$ kcal mol^{–1}). In this case, the vertical/adiabatic S–T gaps decrease to –18.7/–14.9 kcal mol^{–1}. These results are in accordance with those observed when comparing Li₂[**IV**] and [**IV**]^{2–},⁸ and confirm that the beryllole six-electron π cloud is strongly stabilised by the counteranions.

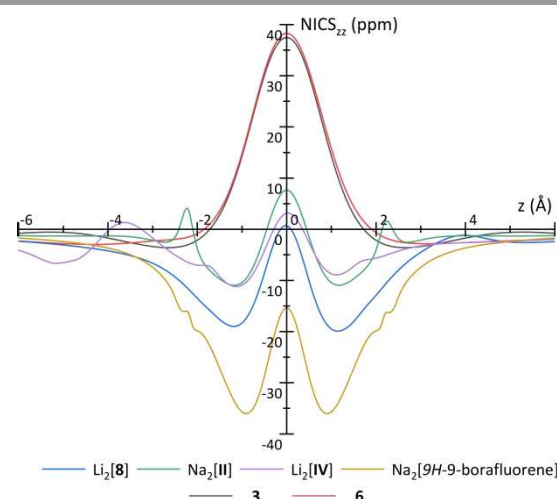


Figure 5. Scan of the *zz* components of the nucleus-independent chemical shifts (NICS_{zz}-scan) of Li₂[**8**], Na₂[**II**], Li₂[**IV**], Na₂[9H-9-borafluorene], and the compounds **3** and **6**.

The NICS_{zz}-scan^{22,23} analysis for Li₂[**8**] (Fig. 5) provides a NICS_{zz}(–1/+1) value of –18.4/–19.6 ppm, which is more negative than those of the beryllole dianion Li₂[**IV**], NICS_{zz}(–1/+1) = –11.0/–8.8 ppm, and the borole dianion Na₂[**II**], NICS_{zz}(–1/+1) = –10.5/–10.5 ppm. In comparison, the NICS_{zz}(–1/+1) values for Na₂[9H-9-borafluorene] and the fluorenyl anion are –35.8/–35.8 and –35.5/–35.5 ppm, respectively. These results demonstrate that the beryllole ring of Li₂[**8**] has a distinct aromatic character, albeit naturally weaker than that of its corresponding boron and carbon analogues. In contrast, the NHC- and CAAC-stabilised compounds **3** and **6** show a strong antiaromatic behaviour of the beryllole rings with NICS_{zz}(–1/+1) values of 14.3/14.3 ppm and 14.8/15.7 ppm, respectively.

The ACID plot of Li₂[8], which enable the evaluation of delocalisation, conjugation and aromaticity,^{24,25} shows a diatropic (clockwise) π -electron circulation characteristic of aromatic molecules (Fig. 4b), consistent with the NICS_{zz} results. At an isovalue of 0.02, no contribution of the beryllium atom to cyclic conjugation is observed, with the π -electron circulation spanning both benzo groups. This highlights the smaller contribution of the alkaline-earth element to cyclic conjugation compared to, for instance, the 9H-9-borafluorene dianion, a feature also observed for Li₂[IV] and its isoelectronic analogues, and in agreement with the lower aromaticity of beryllium metalloles.

In summary, the first six members of the dibenzoberyllole family of compounds were synthesised, three of which were prepared by Lewis base exchange at the beryllium atom of a DBBe diethyl etherate precursor. The compounds were characterised by NMR spectroscopy and X-ray crystallography, and their electronic structures analysed by DFT calculations. The thermal decomposition of the CAAC-stabilised DBBe resulted in a remarkably selective double ring-expansion involving the breaking and making of eight bonds in total and yielded the second known example of a side-on beryllium π complex. Finally, the two-electron reduction of the CAAC derivative yielded the first example of a beryllium-containing aromatic polycyclic species.

Conflicts of interest

There are no conflicts to declare.

Acknowledgements

The authors gratefully acknowledge financial support from the Deutsche Forschungsgemeinschaft (grant numbers BR1149 25-1 and 466754611). F.F. thanks the Coordenação de Aperfeiçoamento de Pessoal de Nível Superior (CAPES) and the Alexander von Humboldt (AvH) Foundation for a Capes-Humboldt postdoctoral fellowship. L.E. thanks the Fonds der Chemischen Industrie (FCI) for a Kekulé fellowship.

Notes and references

† NMR spectra of the crude reaction products show high selectivity for the desired adducts (>85%). The mediocre isolated yields of some compounds are due to difficulties separating these from unknown decomposition and side-products by fractional crystallisation.

- X. Su, T. A. Bartholome, J. R. Tidwell, A. Pujol, S. Yruegas, J. J. Martinez and C. D. Martin, *Chem. Rev.*, 2021, **121**, 4147–4192.
- For general reviews see: a) J. J. Eisch, *Adv. Organomet. Chem.*, 1996, **39**, 355–391; b) A. Steffen, R. M. Ward, W. D. Jones and T. B. Marder, *Coord. Chem. Rev.*, 2010, **254**, 1950–1976; c) H. Braunschweig and T. Kupfer, *Chem. Commun.*, 2011, **47**, 10903–10914; d) H. Braunschweig, I. Kruppenacher and J. Wahler, *Adv. Organomet. Chem.*, 2013, **61**, 1–53; e) H. Braunschweig and I. Kruppenacher, *Organic Redox Systems: Synthesis, Properties, and Applications*, John Wiley & Sons, Hoboken (New Jersey), 2016, 503–519; f) J. H. Barnard, S. Yruegas, K. Huang and C. D. Martin, *Chem. Commun.*, 2016, **52**, 9985–9991; g) B. Su and R. Kinjo, *Synthesis*, 2017, 2985–3034; h) L. Ji, S. Griesbeck and T. B. Marder, *Chem. Sci.*, 2017, **8**, 846–863; i) A. Wakamiya, *Main Group Strategies towards Functional Hybrid Materials*, John Wiley & Sons Ltd, Hoboken (New Jersey), 1st edn, 2018, 1–26; j) Y. Su and R. Kinjo, *Chem. Soc. Rev.*, 2019, **48**, 3613–3659; k) J. He, F. Rauch, M. Finze and T. B. Marder, *Chem. Sci.*, 2021, **12**, 128–147.
- K. R. Bluer, L. E. Laperriere, A. Pujol, S. Yruegas, V. A. K. Adiraju and C. D. Martin, *Organometallics*, 2018, **37**, 2917–2927.
- X. Chen, G. Meng, G. Liao, F. Rauch, J. He, A. Friedrich, T. B. Marder, N. Wang, P. Chen, S. Wang and X. Yin, *Chemistry*, 2021, **17**, 6274–6282.
- M. Lorenz–Rothe, K. S. Schellhammer, T. Jägeler–Hoheisel, R. Meerheim, S. Kraner, M. P. Hein, C. Schünemann, M. L. Tietze, M. Hummert, F. Ortman, G. Cuniberti, C. Körner and K. Leo, *Adv. Electron. Mater.*, 2016, **2**, 1600152.
- U. M. Dzhemilev, A. G. Ibragimov, V. A. D'yakonov and R. A. Zinnurova, *Russ. J. Org. Chem.*, 2007, **43**, 176–180.
- J. Wei, L. Liu, M. Zhan, L. Xu, W.–X. Zhang and Z. Xi, *Angew. Chem. Int. Ed.*, 2014, **53**, 5634–5638.
- D. K. Roy, T. Tröster, F. Fantuzzi, R. D. Dewhurst, C. Lenczyk, K. Radacki, C. Prankevicus, B. Engels and H. Braunschweig, *Angew. Chem. Int. Ed.*, 2021, **60**, 3812–3819.
- J. K. Buchanan and P. G. Plieger, *Z. Naturforsch.*, 2020, **75b**, 459–472.
- a) M. Müller and M. R. Buchner, *Chem. Eur. J.*, 2020, **26**, 9915–9922; b) N. A. Bellan, W. Nowell, G. E. Coates and H. M. M. Shearer, *J. Organomet. Chem.*, 1984, **273**, 179–185; c) B. Morosin and J. Howatson, *J. Organomet. Chem.*, 1971, **29**, 7–14; d) A. I. Snow and R. E. Rundle, *Acta Cryst.*, 1951, **4**, 348–352.
- L. Kaufmann, H. Vitze, M. Bolte, H.–W. Lerner and M. Wagner, *Organometallics*, 2008, **27**, 6215–6221.
- a) M. Arrowsmith, G. Kociok–Kohn, D. J. MacDougall, M. F. Mahon and M. S. Hill, *Angew. Chem. Int. Ed.*, 2012, **51**, 2098–2100; b) M. Arrowsmith, G. Kociok–Kohn and M. S. Hill, *Organometallics*, 2015, **34**, 653–662; c) J. Gottfriedsen and S. Blaurock, *Organometallics* 2006, **25**, 3784–3786.
- M. Niemeyer and P. P. Power, *Inorg. Chem.*, 1997, **36**, 4688–4696.
- M. Arrowsmith, J. Böhnke, H. Braunschweig and M. A. Celik, *Angew. Chem. Int. Ed.*, 2017, **56**, 14287–14292.
- K. C. Mondal, P. P. Samuel, H. W. Roesky, R. R. Aysin, L. A. Leites, S. Neudeck, J. Lübbers, B. Ditrlich, N. Holzmann, M. Hermann and G. Frenking, *J. Am. Chem. Soc.*, 2014, **136**, 8919–8922.
- A. F. Eichhorn, S. Fuchs, M. Flock, T. B. Marder and U. Radius, *Angew. Chem. Int. Ed.*, 2017, **56**, 10209–10213.
- a) G. Wang, J. E. Walley, D. A. Dickie, A. Molino, D. J. D. Wilson and R. J. Gilliard Jr., *Angew. Chem. Int. Ed.*, 2021, **60**, 9407–9411; b) D. Naglav, A. Neumann, D. Bläser, C. Wölper, R. Haack, G. Jansen and S. Schulz, *Chem. Commun.*, 2015, **51**, 3889–3891.
- S. Gonell, E. A. Assaf, K. D. Duffee, C. K. Schauer and A. J. Miller, *J. Am. Chem. Soc.*, 2020, **142**, 8980–8999.
- A. Paparo, A. J. R. Matthews, C. D. Smith, A. J. Edwards, K. Yuvaraj and C. Jones, *Dalton Trans.*, 2021, **50**, 7604–7609.
- G. Knizia, *J. Chem. Theory Comput.*, 2013, **9**, 4834–4843.
- J. Gilmer, H. Budy, T. Kaese, M. Bolte, H.–W. Lerner and M. Wagner, *Angew. Chem. Int. Ed.*, 2020, **59**, 5621–5625.
- J. O. C. Jiménez-Halla, E. Matito, J. Robles and M. Solà, *J. Organomet. Chem.*, 2006, **691**, 4359–4366.
- A. C. Tsipis, *Phys. Chem. Chem. Phys.*, 2009, **11**, 8244.
- D. Geuenich, K. Hess, F. Köhler and R. Herges, *Chem. Rev.*, 2005, **105**, 3758–3772.
- R. Herges and D. Geuenich, *J. Phys. Chem. A*, 2001, **105**, 3214–3220.